geologica acta

Citation: Domínguez-Carretero, D., Villanova-de-Benavent, C., Torró, L., Pujol-Solà, N., Bover-Arnal, T., Mestre, À., Aiglsperger, T., Ramírez, A., Rodríguez, J., Espaillat, J., Proenza, J.A., 2025. Mineralogy, geochemistry and origin of karst bauxite deposits from the Reserva Fiscal Ávila, SW Dominican Republic. Geologica Acta, 23.9, 1-17. Online ISSN: 1696-5728 DOI: 10.1344/GeologicaActa2025.23.9

Mineralogy, geochemistry and origin of karst bauxite deposits from the Reserva Fiscal Ávila, SW Dominican Republic

Diego Domínguez-Carretero[1] Cristina Villanova-de-Benavent[1] Lisard Torró[2] Núria Pujol-Solà[3] Telm Bover-Arnal[1] Àngel Mestre[1] Thomas Aiglsperger[4] Australia Ramírez[5] Jesús Rodríguez[5] Julio Espaillat[6] Joaquín A. Proenza[1]

[1]Departament de Mineralogia, Petrologia i Geologia Aplicada, Facultat de Ciències de la Terra, Universitat de Barcelona
Marí i Franquès s/n, 08028, Barcelona. Domínguez-Carretero E-mail: ddominguezcarretero@gmail.com Villanova-de-Benavent E-mail: cvillanovadb@ub.edu Bover-Arnal E-mail: telm.boverarnal@ub.edu Mestre E-mail: mestreangel2001@gmail.com Proenza E-mail: japroenza@ub.edu

[2]Geological Engineering Program, Faculty of Sciences and Engineering, Pontifical Catholic University of Peru
Lima, Perú. E-mail: ltorro@pucp.edu.pe

[3]Departamento de Mineralogía y Petrología, Facultad de Ciencias, Universidad de Granada
Granada, Spain. E-mail: npujolsola@ugr.es

[4]Dept. Civil Engineering and Natural Resources, Division of Geosciences and Environmental Engineering, Luleå University of Technology
Luleå, Sweden. E-mail: thomas.aiglsperger@ltu.se

[5]Servicio Geológico Nacional
Av. Winston Churchill 75, Edificio "J. F. Martínez", Santo Domingo, Dominican Republic. Ramírez E-mail: aramirez@sgn.gob.do Rodríguez E-mail: jrodriguez@sgn.gob.do

[6]Ministerio de Energía y Minas
Av. Independencia 1428, Centro de los Héroes, Santo Domingo, Dominican Republic. Espaillat E-mail: julio.espaillat@mem.gob.do

ABSTRACT

The energy transition, which aims to reduce carbon emissions and to slow down climate change, demands an ever-increasing supply of the so-called "critical metals". Rare-earth Elements and Yttrium (REY) are among the most critical metals, as they are indispensable in most technologies associated with the generation and storage of renewable energy. In recent years there has been a growing interest in the potential of karst bauxites as non-conventional sources of REY and other critical metals such as Sc and Ga. The Sierra de Bahoruco (SW Dominican Republic) contains the most REY-enriched karst bauxites globally. In view of the high potential for hosting important REY contents, the Dominican Republic government has declared the Reserva Fiscal Ávila (RFA), a state-owned area within the Sierra de Bahoruco for assessment and exploration of its REY resources. In this study, we present the first data on the mineralogy and composition of bauxitic rocks from the RFA. The bauxitic deposits comprise clayey bauxites and Fe-rich bauxites that are composed predominantly of Al-oxyhydroxides (gibbsite, boehmite and nordstrandite), kaolinite and Fe-oxyhydroxides. The bauxites are enriched in REY, with a median value of 1,310ppm and up to 2,542ppm, with a consistent enrichment in light REE (LREE) and Y compared to middle (MREE) and heavy REE (HREE). The positive correlation between the contents of REY and Th, and negative correlation with K, makes gamma-ray spectrometry an appropriate tool for the exploration. In addition, bauxitic rocks from the RFA contain significant Sc (up to 105ppm) and Ga (up to 54ppm) contents, and their extraction could potentially represent a substantial economic surplus to the revenue generated solely from the aluminum production.

KEYWORDS **Karst bauxite. Critical metals. Rare-earth Elements and Yttrium (REY). Dominican Republic. Caribbean.**

INTRODUCTION

The last Climate Summit (COP28) held in Dubai in December 2023 was marked by an unprecedented call for an energy transition that should cut off coal, oil and gas, in order to slow down climate change. However, the deployment of low-carbon energy technologies is expected to result in a significant surge in the demand for minerals (European Commission, 2023; International Energy Agency, 2023; International Renewable Energy Agency, 2023). The energy transition to renewable energies will only be possible if there is security in the supply chains of the so-called "critical metals" (European Commission, 2023; Herrington *et al.*, 2021). The criticality of these metals resides in whether they are essential for modern technologies, economies and national security, yet their supply chains are susceptible to disruption.

Among the most critical metals are the Rare-earth Elements and Yttrium (REY). While REY were previously extracted in limited quantities, their unique physical-chemical properties have made them indispensable in technologies associated with renewable energy production, greenhouse gas emissions reduction, and energy efficiency (Balaram, 2019; Charles *et al.*, 2021; Goodenough *et al.*, 2017). Currently, worldwide, there are only eleven significant active REY mines and seven processing plants (six of them in China). Despite this, the global REY mining production increased from 110,000 tons in 2013 to 300,000 tons in 2022 (USGS, 2024). In response to the growing demand, numerous exploration projects are underway, mostly in Canada, the United States, Russia, Australia, Norway, South Africa and other African countries (Liu *et al.*, 2023).

The ever-increasing interest in REY has led to the identification of the so-called "non-conventional" REY deposits, which include karst bauxites. Karst bauxites, especially those belonging to the Mediterranean subtype, described by Bárdossy (1982) as "karst bauxites in the strict sense" meaning that these represent the classic model for karst-bauxite deposits, are typically well-defined karst infills with a wide variety of sizes and shapes, may contain 100s to few 1000s of ppm of REY (*e.g.* Deady *et al.*, 2014; Mondillo *et al.*, 2011, 2019; Mouchos *et al.*, 2016; Putzolu *et al.*, 2018; Radusinovic and Papadopoulos, 2021; Reinhardt *et al.*, 2018), making them attractive targets for REY exploration. The most REY-enriched karst bauxites in the world are found in the Sierra de Bahoruco (SW Dominican Republic), with average REY contents of 1,900ppm (Proenza *et al.*, 2017; Torró *et al.*, 2017; Villanova-de-Benavent *et al.*, 2023). In particular, specific karst bauxite deposits of the Sierra de Bahoruco yield REY contents exceeding 2wt.%, representing the highest recorded contents in karst bauxite materials (Villanova-de-Benavent *et al.*, 2023). Due to the high potential of the Sierra de Bahoruco to host significant REY mineralization, the government of the Dominican Republic issued the Decree 430-18, declaring the Reserva Fiscal Ávila (RFA), a state-owned area situated in the westernmost portion of the Bahoruco mountain range, as a region warranting exploration and assessment for REY resources.

This contribution presents the first detailed petrographic and geochemical characterization of a representative selection of bauxitic deposits distributed throughout the RFA. This study is primarily concerned with constraining the geochemistry of the bauxites in order to address the potential of the RFA to host significant REY and other critical metals (*e.g.* Sc and Ga) resources. The trace elements composition is also used to shed light on the possible parental source of the RFA bauxites.

GEOLOGICAL SETTING

The RFA covers ~20x14km along the Pedernales peninsula in the SW of the Dominican Republic. The area is limited to the East by the Sierra de Bahoruco National Park and to the West by the Pedernales river, which also delineates the border with Haiti (Fig. 1).

The karst bauxites in the Pedernales peninsula are hosted by different Eocene to Quaternary carbonate units including the Aceitillar and Neiba formations (lower Eocene-Oligocene), the Aguas Negras, Pedernales, and Barahona units (upper Oligocene-Miocene), the La Cueva Unit (Pliocene-lower Pleistocene), and lagoon and pocket beach carbonates (Pleistocene-Holocene). These units overlie the Campanian to lower Eocene volcanic Dumisseau Formation, which consists of basaltic flows, pyroclastic deposits and lesser sedimentary deposits representing an on-land portion of the Caribbean Large Igneous Province (Escuder-Viruete, 2010; Escuder-Viruete *et al.*, 2016; Lidiak and Anderson, 2015). The carbonate sequence records a progressive shift in depositional environments from deep, outer slope settings during the Eocene, through shallow, inner platform and reef-boundstone deposition in the Pliocene, to emersion in the Pleistocene (de León, 1989; Pérez-Valera, 2010; Pérez-Valera and Abad, 2010).

The uplift and deformation in the Bahoruco Peninsula started in the Pliocene as a consequence of the oblique convergence of the North American plate continental margin and the Caribbean island arc (Mann, 2007; Pérez-Valera, 2010). This led to the formation of high-angle reverse and strike-slip faults, as well as soft, kilometric-scale folds, which produced rugged relief and exposed the carbonate units, causing widespread karstification. The resulting karst landforms and paleo-erosion surfaces now

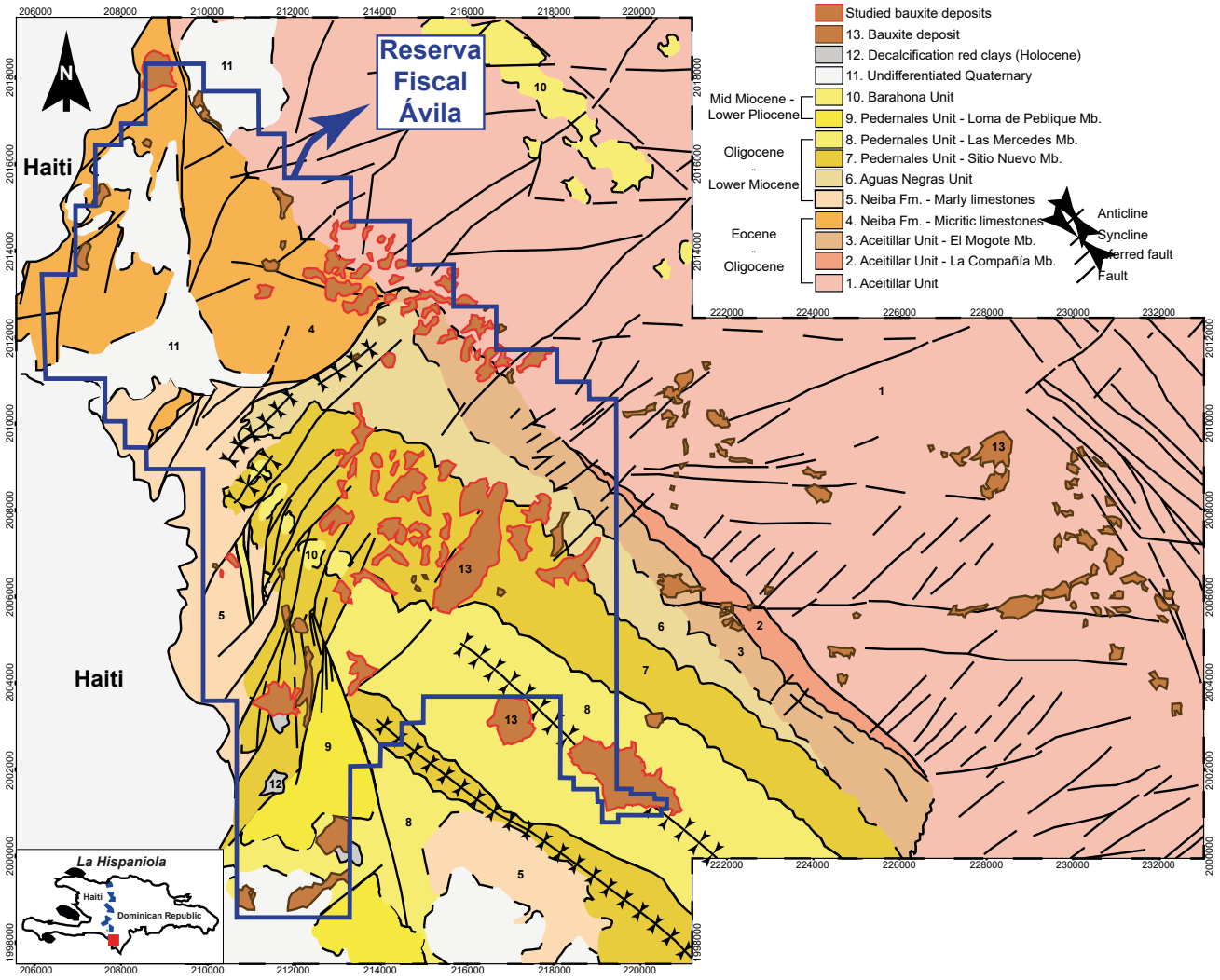

FIGURE 1. Geological map of the RFA within the Sierra de Bahoruco. Modified from Mendoza-Ulloa *et al.* (2023).

contain Pleistocene-Holocene decalcification red clays and bauxite argillizations (Pérez-Valera, 2010), thanks to repeated sea-level highstands, promoting the development of alteration profiles and karsitification, and lowstands combined with the uplift of the Sierra de Bahoruco ranges, favouring erosion of alteration surfaces, transport and deposition in depressed landforms (*e.g.* Moseley *et al.*, 2015; Thompson *et al.*, 2011).

The studied karst bauxite deposits from the RFA are hosted by the Aceitillar Unit, which also hosts the Km-30 and Aceitillar deposits described in Villanova-de-Benavent *et al.* (2023), the Neiba Formation, the Aguas Negras Unit, and the Pedernales Unit (Sitio Nuevo and Las Mercedes members; Figs. 1; 2; 3A). The Aceitillar Unit (lower-upper Eocene) is composed of homogeneous, oncolytic limestone and comprises two members: the upper La Compañía Member and lower, El Mogote Member. The Neiba Formation (upper Eocene-lower Miocene), in particular the upper member that occurs in the study area, consists of white-beige micritic limestone, with accumulation of bioclasts and silex nodules. The Aguas Negras Unit (upper Oligocene) is composed of beige, poorly organized, silicified limestone with intervals of marly limestone and levels with accumulations of macroforaminifera and, less commonly, massive limestone with silex nodules. The Pedernales Unit corresponds to the so-called "Pedernales limestones" (de León, 1989). The Sitio Nuevo Member (Oligocene-lower Miocene) consists of centimetric levels of white-pinkish, slightly marly limestone with non-parallel, wavy stratification and wackestone texture, containing isolated foraminifera, alternating with decimetric packstone levels with reworked shallow fauna. Finally, the Las Mercedes Member (lower Miocene), is composed of

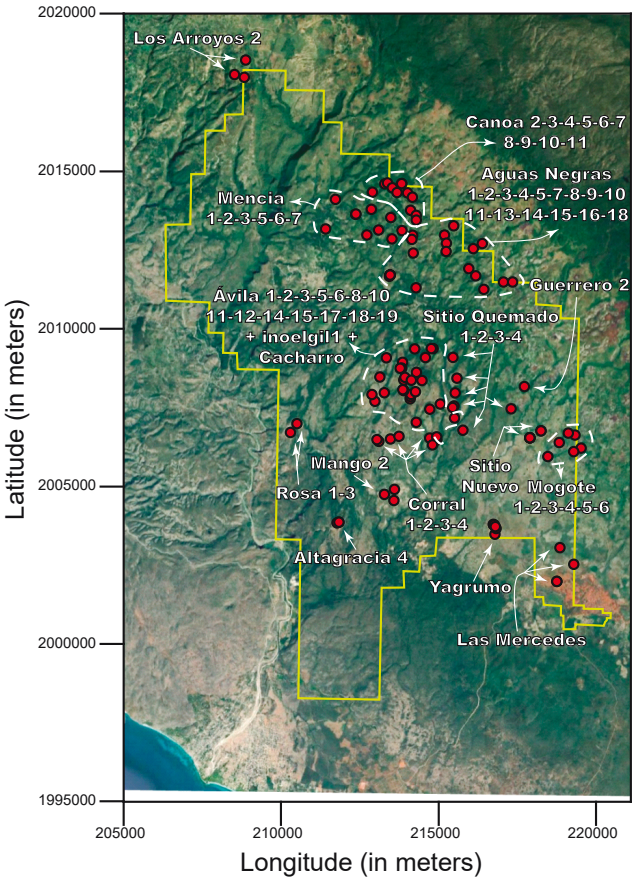

FIGURE 2. Location of the studied bauxite occurrences within the RFA. Satellite image taken from Google Earth.

pinkish limestone with abundant foraminifera, alternating with centimetric levels of marly limestone (Pérez-Valera, 2010). The position of the carbonate units and members is summarized in the stratigraphic column in Figure 3A.

The bauxite deposits fill karst cavities and may be disrupted by carbonate pillars (Fig. 3B). They may reach thicknesses of 15m (Fig. 3C). The bauxitic material is loose, fairly homogeneous, fine-grained and exhibits a distinctive intense reddish-brown color (Fig. 3C-D). It is commonly overlain by up to 2-m-thick bauxitic clays (a.k.a. *terra rossa*).

METHODOLOGY

The geochemical and mineralogical characterization was carried out in 121 samples collected throughout the RFA in different fieldwork campaigns. A total of 70 karst bauxite occurrences were sampled for this study and have been classified geographically in northern, central and southern according to their position within the RFA (Fig. 2). The northern occurrences are: Aguas Negras 1, 2, 3, 4, 5, 7, 8, 9, 10, 11, 13, 14, 15, 16 and 18; Canoa 2, 3, 4, 5, 6, 7, 8, 9, 10 and 11; Guerrero 2; Los Arroyos 2; Mencia 1, 2, 3, 5, 6 and 7. The central occurrences are: Avila 1, 2, 3, 5, 6, 8, 10, 11, 12, 14, 15, 17, 18 and 19; Cacharro; Corral 1, 2, 3 and 4; inoegil 1; Sitio Quemado 1, 2, 3 and 4. Finally, the southern occurrences are constituted by: Altagracia 4; Las Mercedes; Mango 2; Mogote 1, 2, 3, 4, 5 and 6; Rosa 1 and 3; Sitio Nuevo; Yagrumo. The different samples for each deposit and their coordinates are provided in Appendix 1. Twenty-three samples were embedded in Epoxy® resin and prepared as polished thin sections for petrographic microscope and scanning electron microscope (SEM) observations. The SEM used was an Environmental SEM Quanta 200 FEI, XTE 325/D8395 equipped with an INCA Energy 250 EDS microanalysis system (operating conditions: acceleration voltage of 20kV and a beam current of 1nA) at the Centres Científics i Tecnològics of the University of Barcelona (CCiT-UB).

Major, minor and trace element contents were determined at: i) Activation Laboratories Ltd. (Actlabs, Ontario, Canada), where 38 samples were analyzed by means of fusion inductively coupled plasma emission (FUS-ICP) and inductively coupled plasma emission mass spectrometry (ICP-MS) and at ii) ALS (Vancouver, Canada), where 83 samples were analyzed by means of inductively coupled plasma atomic emission spectroscopy (ICP-AES) and by lithium borate fusion ICP-MS. All whole-rock data including element concentrations and detection limits are presented in Appendix I.

Thirty-eight representative samples from different deposits of the RFA were selected for mineralogical characterization. The samples were carefully ground using agate mortar and pestle, and were manually pressed by means of a glass plate to get a flat surface, in cylindrical standard sample holders of 16mm of diameter and 2.5mm of height. Diffractograms were obtained in a Bruker D8 Discover powder diffractometer in Bragg-Brentano θ/2θ geometry with a 240mm radius, nickel-filtered Cu Kα radiation (k= 1.5418Å) and 45kV-40mA at Centro de Caracterización de Materiales of the Pontifical Catholic University of Peru (CAM-PUCP). The software X'Pert HighScore was used to identify, as well as to semiquantitatively determine, the mineral phases present in the powder samples. All X-ray diffraction data and representative patterns are presented in Appendix II and III respectively.

RESULTS

Textures of the bauxitic rocks

The studied deposits consist of red, ochre, and brown unconsolidated bauxites devoid of discernible stratification.

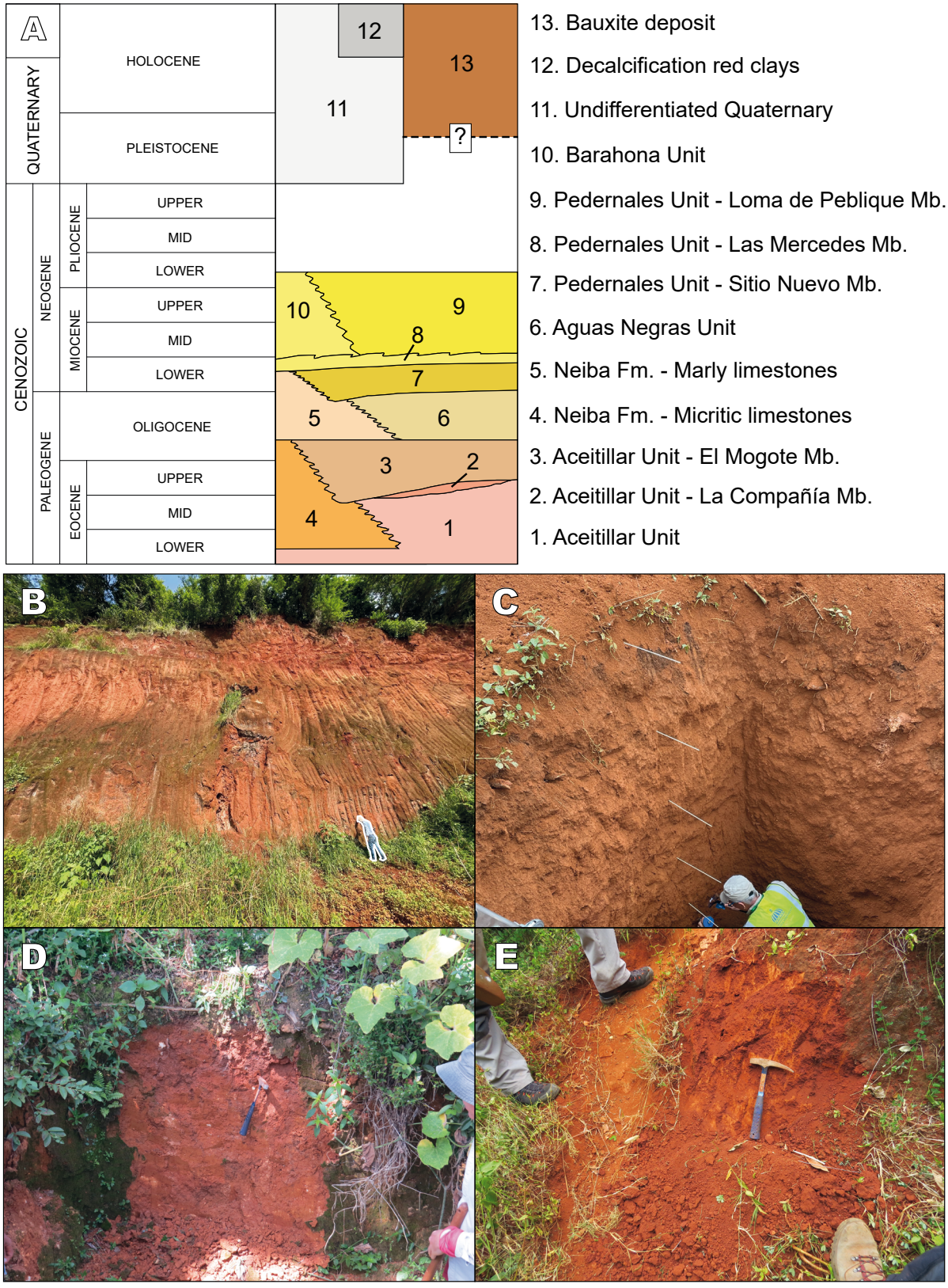

FIGURE 3. A) Schematic lithostratigraphic column of the RFA sedimentary units. Field photographs of (B) the white carbonate columns hosting the bauxite mineralization in Las Mercedes deposit (southern RFA), (C) bauxite outcrop in Las Mercedes deposit (southern RFA) with a thickness over 15 m, (D) bauxite outcrop at Los Arroyos 2 deposit (northern RFA), and (E) bauxite outcrop at Sitio Quemado 3 deposit (central RFA).

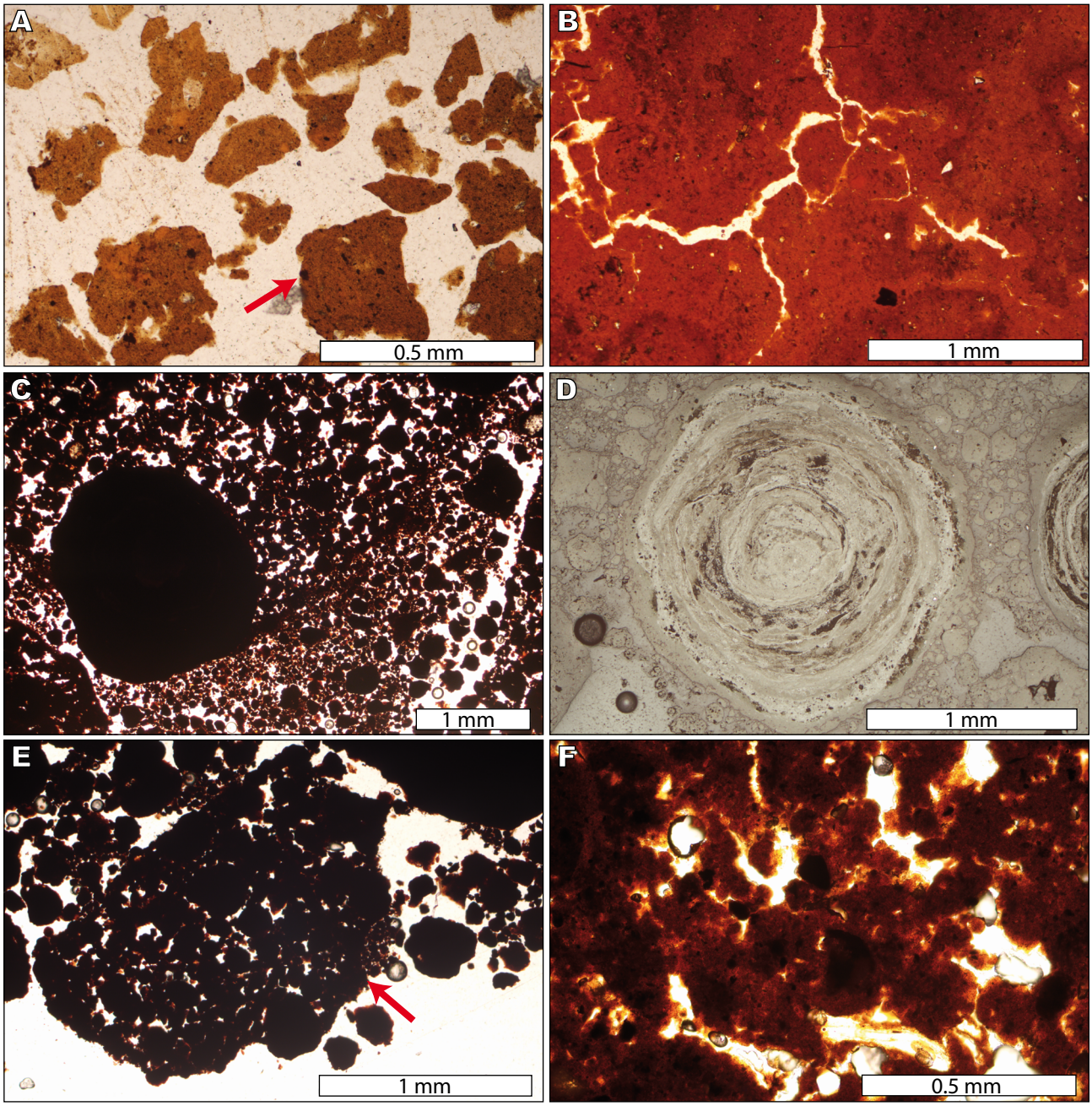

FIGURE 4. Photomicrographs of bauxite particles in transmitted (A-C, E-F) and reflected light (D). A) Sub-rounded to angular-edged micron-sized bauxite particles exhibiting a brown pelitomorphic matrix including darker ferruginous grains (red arrow). B) Close-up view of a relatively homogeneous red pelitomorphic texture intersected by an irregularly branching network of open fissures. C) Detail of loose roundgrains with interiors made up of a homogenous pelitomorphic matrix. D) Close-up view of a pisoid sensu Bárdossy (1982). Note the presence of open fissures and void dissolution of pelitomorphic matrix on the right side of the particle. E) Close-up view of a millimeter-sized ellipsoid-shaped aggregate (red arrow) of roundgrains. F) Example of coalescing clay- and sand-sized grains forming bauxitic masses.

The bauxite lumps easily crumble when handled, resulting in particles primarily ranging from 0.3 to 7mm in diameter (Fig. 4A). However, some slightly compacted bauxite deposits yield larger fragments (Fig. 4B), reaching diameters up to 1.5cm. The bauxite particles typically exhibit sub-rounded to irregular, sharp-edged outlines (Fig. 4A). Additionally, the bauxite deposits comprise roundgrains (*sensu* Bárdossy, 1982) with diameters between 0.3 and 1.5mm (Fig. 4C), as well as ooids and pisoids (Figs. 4D; 5A-B). The roundgrains frequently assemble into ellipsoid-shaped aggregates ranging from 1 to 2mm in diameter (Fig. 4E). The different types of particles are often intersected by

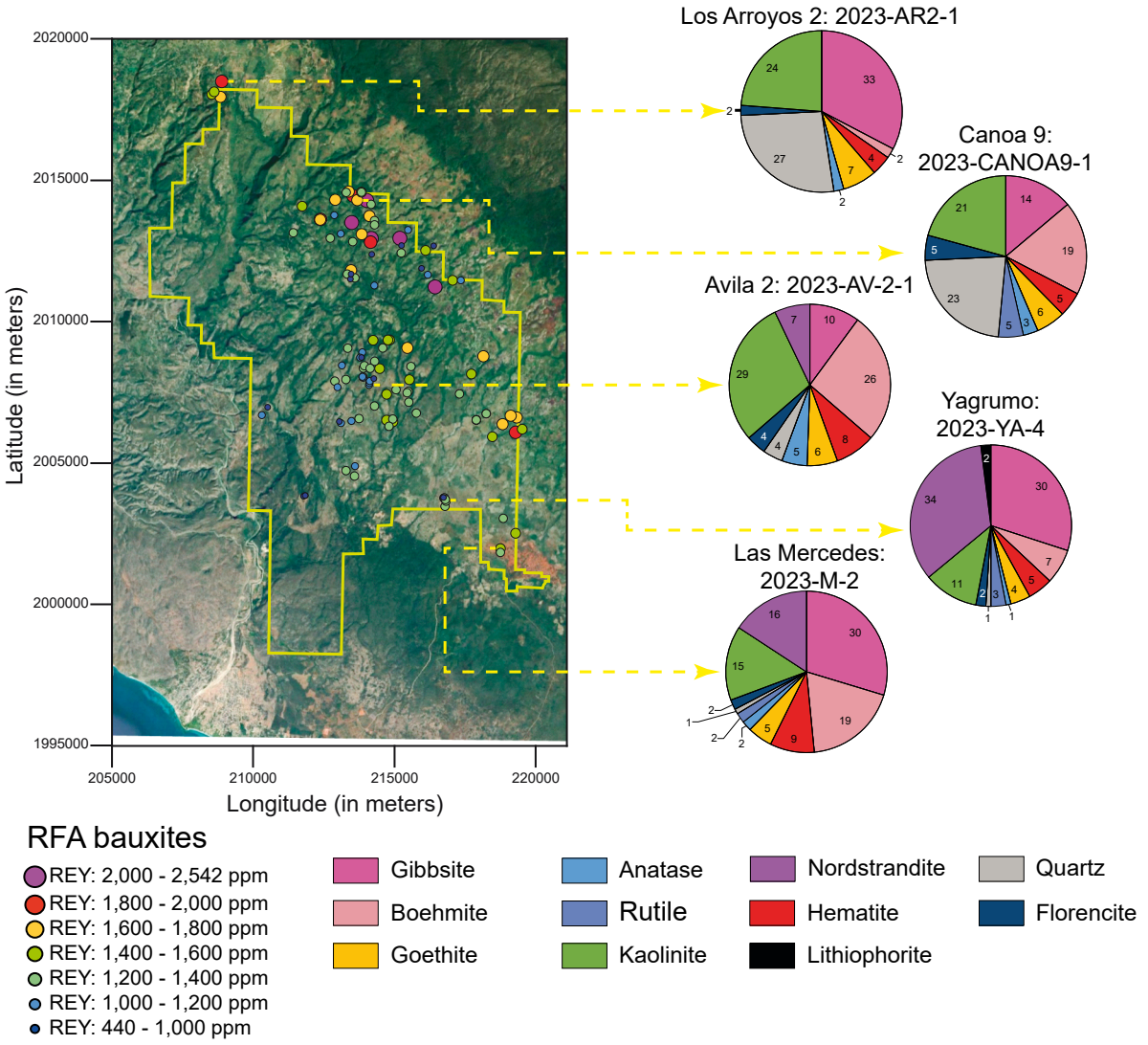

FIGURE 5. Location of the studied bauxite samples within the RFA, together with the quantitative mineralogy of 5 representative bauxite samples distributed throughout the RFA. The samples are color-coded according to their REY contents. Satellite image taken from Google Earth.

irregularly branching fissure networks, most of which are open (Fig. 4B). Some fissures, however, may be occluded by ferruginous cements. Under petrographic examination, the bauxite particles reveal coalescing clay- and minor sand-sized grains (Fig. 4F). The particles exhibit a reddish to brownish pelitomorphic texture (see Bárdossy, 1982), which includes rounded to elongated darker ferruginous grains (Fig. 4A-B, F). Micron-sized void dissolution within the pelitomorphic matrix of the bauxite particles occurs (Fig. 4A-B).

Mineralogy of the bauxite ore

In general, the most abundant phases are kaolinite (9-39modal%) and Al-oxyhydroxides (5-34modal% gibbsite, up to 34 modal % boehmite and up to 50 modal% nordstrandite, another $Al(OH)_3$ polymorph), followed by Fe-oxyhydroxides (2-9modal% hematite and 3-13modal % goethite), and minor TiO_2 (1-5.1modal% anatase and up to 8.1modal% rutile; Fig. 5; Appendix II-III). In all samples a phase with the florencite structure is present in small quantities (1-6.1modal%). Additionally, all the studied deposits, with the exception of Corral 1 and Sitio Quemado 3, contain smectite.

Most of the samples have kaolinite as the main Al phase. The samples in which gibbsite is the predominant Al phase come from Los Arroyos 2, Mencía 1, Sitio Quemado 3, Las Mercedes and Yagrumo. Conversely, boehmite is dominant in Canoa 10, and the Ávila 1, 2, 3, 8, 14 and 15 deposits. With few exceptions, gibbsite is more abundant than boehmite in the northern and

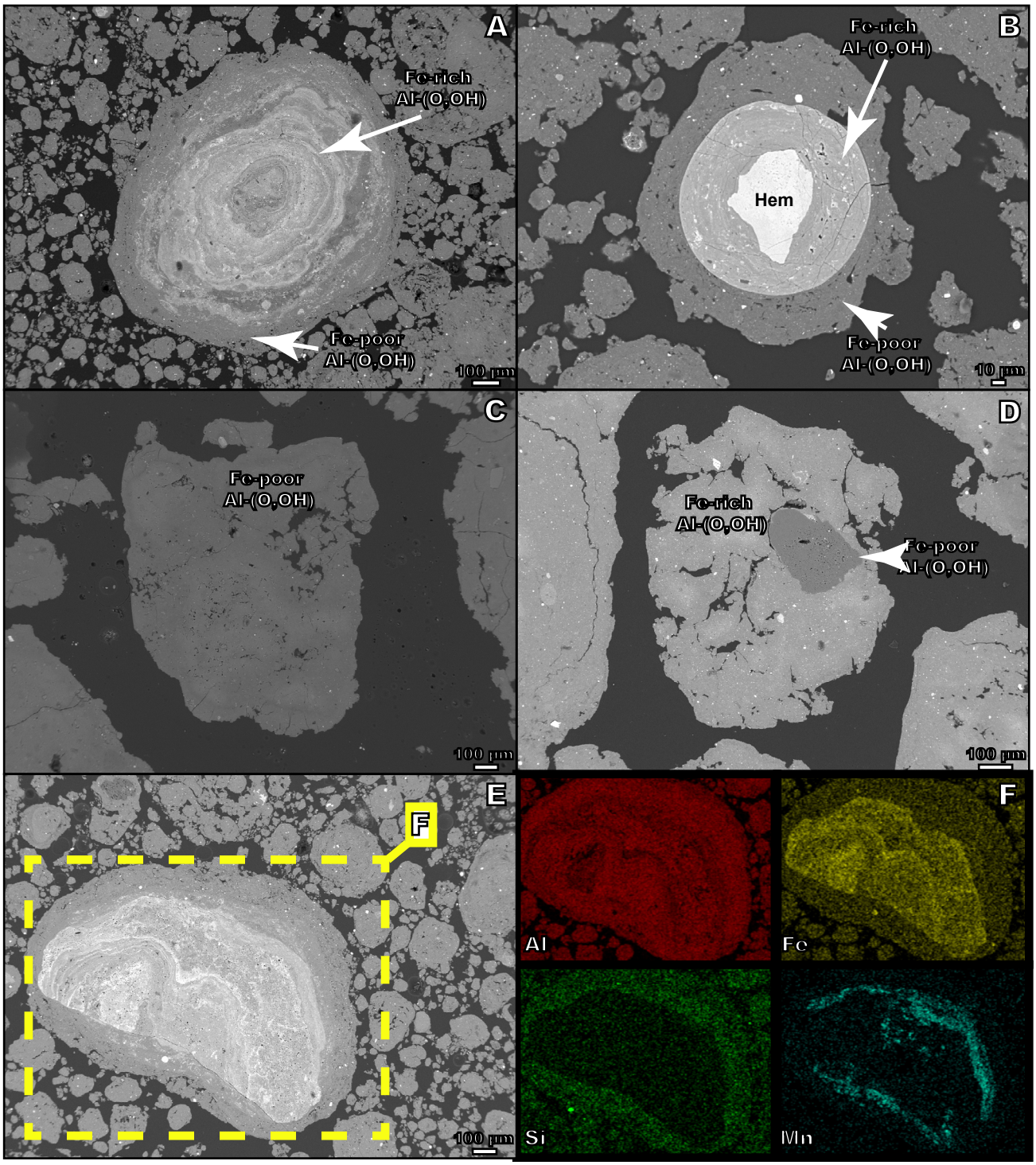

FIGURE 6. Back-Scattered Electron (BSE) images of A) a pisoid constituted by Al-oxyhydroxides; B) a pisoid whose core is composed of hematite and is later surrounded by Al-oxyhydroxides, included within a fine-grained pelitomorphic matrix; C-D) pelitomorphic texture matrix, the brighter, smaller particles being constituted by fine-grained hematite and/or anatase; E) roundgrain with oscillatory zoning; and F) EDS Al, Fe, Si, and Mn elemental maps of the roundgrain in (E). Abbreviations: Al-(O,OH)= Al-oxyhydroxide.

southern areas and is less abundant than boehmite in the central area.

The deposits in which nordstrandite has been identified include Ávila 1, 2, 3, 8 and 15; Corral 1; Altagracia 4; Las Mercedes; Yagrumo. The highest amounts of this mineral were found in the southernmost part of the RFA (Yagrumo).

The deposits from the northern area (Los Arroyos 2; Aguas Negras 13, 14; Canoa 6, 9, 10; Mencía 1, 2, 5) are characterized by the prevalence of goethite over hematite. In contrast, the remaining deposits exhibit a greater abundance of hematite, which is either larger than or very similar in quantity to that of goethite. With regard to quartz, most deposits contain less than 10modal% of this mineral (Canoa 6; Mencía 2, Ávila 1, 2, 3, 8, 14, 15; Cacharro; Corral 1; Inoel Gil; Sitio Quemado 3; Altagracia 2, 4; Las Mercedes, Yagrumo). However, certain deposits, concentrated in the northernmost area of the RFA, have between 14 and 38modal% quartz (Canoa 9, 10; Aguas Negras, 13, 14; Mencía 1, 5), with some reaching 66-67modal% quartz (Los Arroyos 2).

Back-Scattered Electron (BSE) images reveal that pisoids and ooids are internally heterogeneous and exhibit cores with fine concentric zonation (Fig. 6A, E), which largely corresponds to variable Al, Fe^{3+} and Mn contents (Fig. 6F). In some instances, hematite aggregates constitute the nucleus of these grains (Fig. 6B). Minute anatase and hematite grains are scattered in the pelitomorphic matrix (Fig. 6C-D).

Geochemistry

Major and trace element geochemistry and geochemical classification

The studied bauxite samples (n= 121) contain variable Al_2O_3 (16.4 to 48.2wt.%, median of 37.4wt.%), Fe_2O_3 (4.41 to 26.2wt.%, median of 17.9wt.%) and SiO_2 (3.55 to 51.6wt.%, median of 17.4wt.%) contents. Additionally, all samples contain considerable amounts of TiO_2 (0.53 to 2.78wt.%, median of 2.00wt.%) and P_2O_5 (0.86 to 7.09wt.%, median of 3.06wt.%), and low CaO contents (0.19 to 4.7wt.%, median of 1.11 wt.%). In the Al_2O_3-Fe_2O_3-SiO_2 ternary diagram proposed by Bárdossy (1982), the RFA samples are mostly classified as clayey bauxites, Fe-rich bauxites and bauxites *sensu stricto* (Fig. 7A), which is consonant with moderate to strong weathering according to the compositional fields of Chen *et al.* (2018) (Fig. 7B). Two samples from the northernmost deposit of Los Arroyos 2 are classified as bauxitic clays due to their differential enrichment in silicates.

The studied samples show general positive correlation trends between Al_2O_3 and Fe_2O_3, as well as TiO_2, and good negative correlation (R^2= 0.79) with SiO_2 (Fig. 8). These results suggest that SiO_2 becomes progressively depleted, and Al_2O_3, Fe_2O_3 and TiO_2 more enriched, during the bauxitization process. The analyzed bauxites have also high contents of Zr (median contents of 343ppm, and up to 543ppm), V (median contents of 277ppm, and up to 698ppm), Sc (median contents of 66ppm, and up to 105ppm), Ga (median contents of 40ppm, and up to 54ppm) and Th

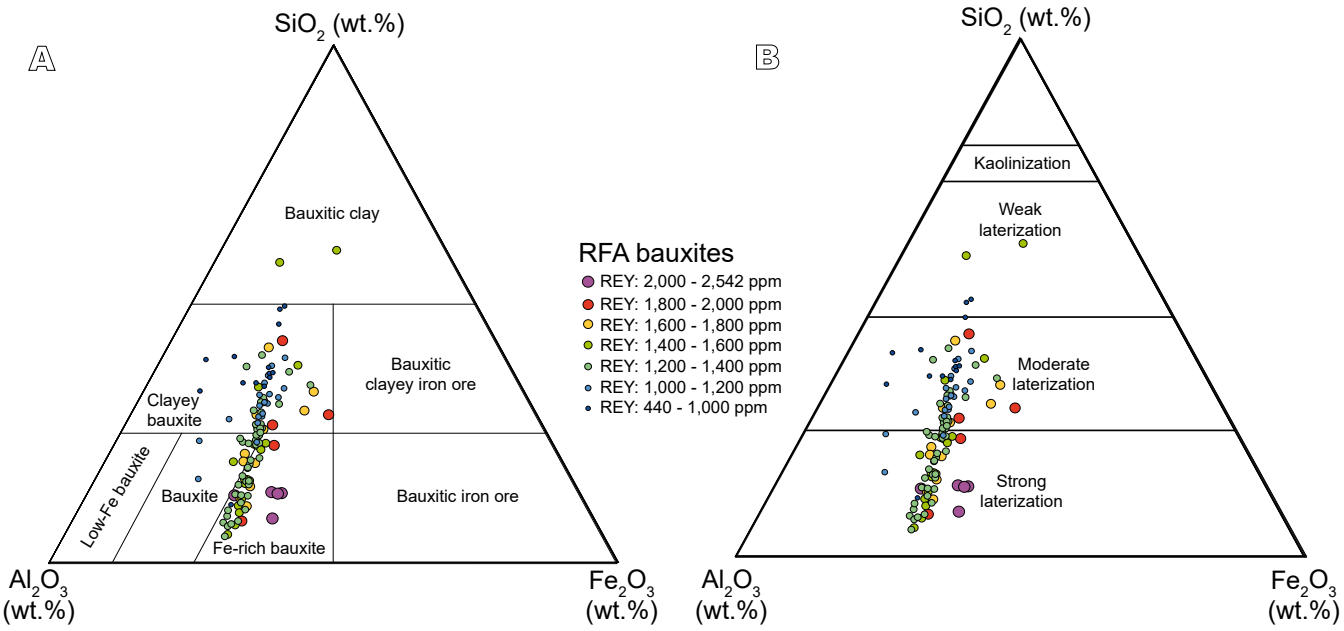

FIGURE 7. Whole rock Al_2O_3-SiO_2-Fe_2O_3 ternary plots of the studied bauxites. Bauxite classification fields are from A) Bárdossy (1982) and B) Chen *et al.* (2018).

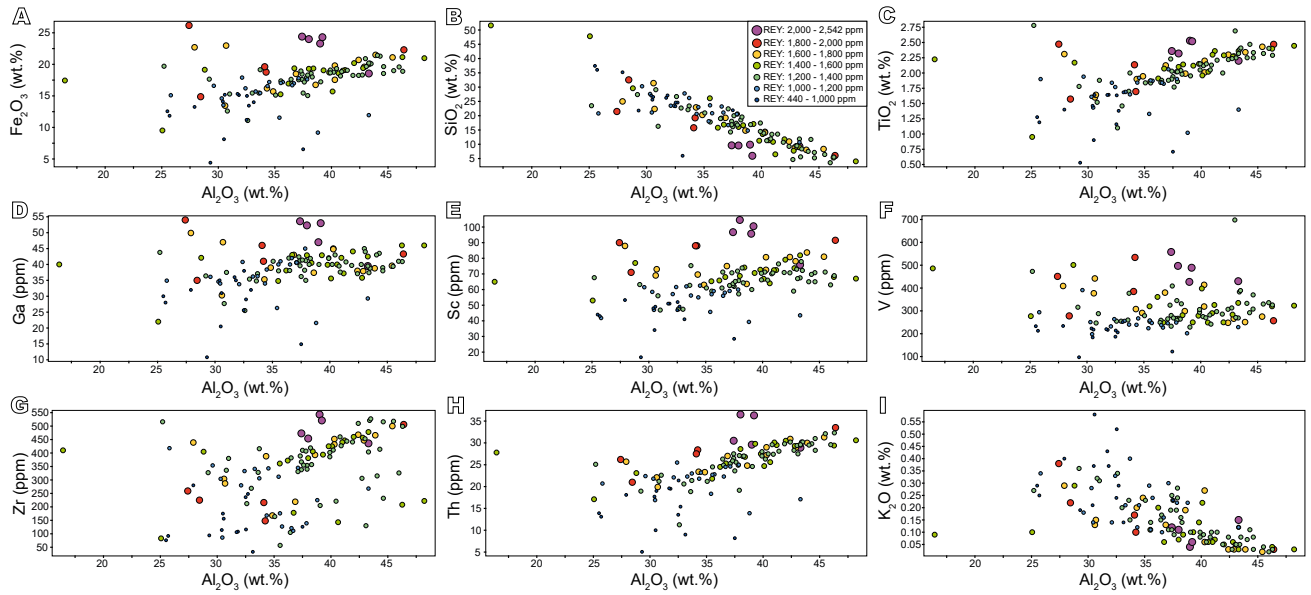

FIGURE 8. Whole-rock binary diagrams of Al_2O_3 (wt.%) vs A) Fe_2O_3 (wt.%), B) SiO_2 (wt.%), C) TiO_2 (wt.%), D) Ga (ppm), E) Sc (ppm), F) V (ppm), G) Zr (ppm), H) Th (ppm) and I) K_2O (wt.%).

(median contents of 26ppm, and up to 37ppm). Al_2O_3 has moderate positive and negative correlations with Th (R^2= 0.40) and K_2O (R^2= 0.42), respectively (Fig. 8).

REE + Y geochemistry

The studied bauxite samples from the RFA are systematically REY-rich, with a median content of 1,310ppm, and minimum and maximum contents of 440ppm and 2,542ppm, respectively. Geographically, the most REY-enriched samples are situated towards the northernmost areas of the RFA (Fig. 5) and are classified as Fe-rich bauxites (Fig. 7). The REY content of the RFA bauxites is independent of the Al_2O_3 values (Fig. 9A), however, it appears that, in broad terms, the lower SiO_2 in the samples, the higher REY they contain (Figs. 7; 9C). Additionally,

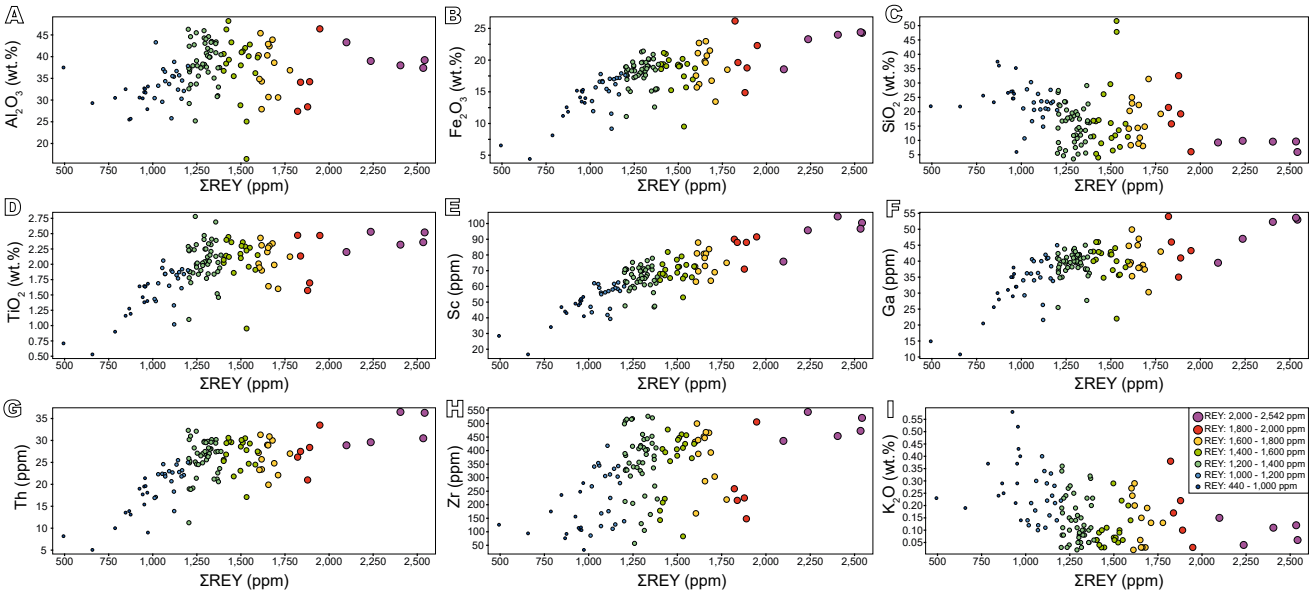

FIGURE 9. Whole-rock binary diagrams of REY (ppm) vs A) Al_2O_3 (wt.%), B) Fe_2O_3 (wt.%), C) SiO_2 (wt.%), D) TiO_2 (wt.%), E) Sc (ppm), F) Ga (ppm), G) Zr (ppm), H) Th (ppm) and I) K_2O (wt.%).

REY present general positive correlations with Fe_2O_3, TiO_2, Sc, Ga, Th and Zr, and negative correlations with K_2O (Fig. 9). All the bauxite samples are more enriched in LREE (La to Nd; median content of 753ppm) than in MREE (Sm to Gd; median content of 88ppm) and HREE (Tb to Lu; median content of 106ppm), and have median Y contents of 371ppm. The chondrite-normalized REY plot for the studied samples exhibits linear negative slope patterns and systematic negative Ce and Eu anomalies, with Ce/Ce* and Eu/Eu* ratios of 0.34 to 0.71 and 0.61 to 0.83, respectively (Fig. 10).

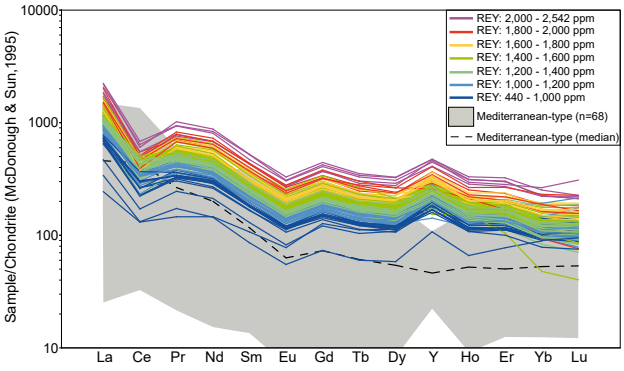

FIGURE 10. Chondrite-normalized REY spider diagram of the studied bauxites. Normalization values are after McDonough and Sun (1995). Data are compared to REY values from Mediterranean-type bauxites (Deady *et al.*, 2014; Mondillo *et al.*, 2011, 2019; Mouchos *et al.*, 2016; Putzolu *et al.*, 2021; Radusinovic and Papadopoulos, 2021; Reinhardt *et al.*, 2018).

DISCUSSION

Bauxite formation and source material

One of the primary challenges in understanding the genesis of bauxite deposits hosted within karst systems is determining the origin and accumulation of Al, Si, Fe,

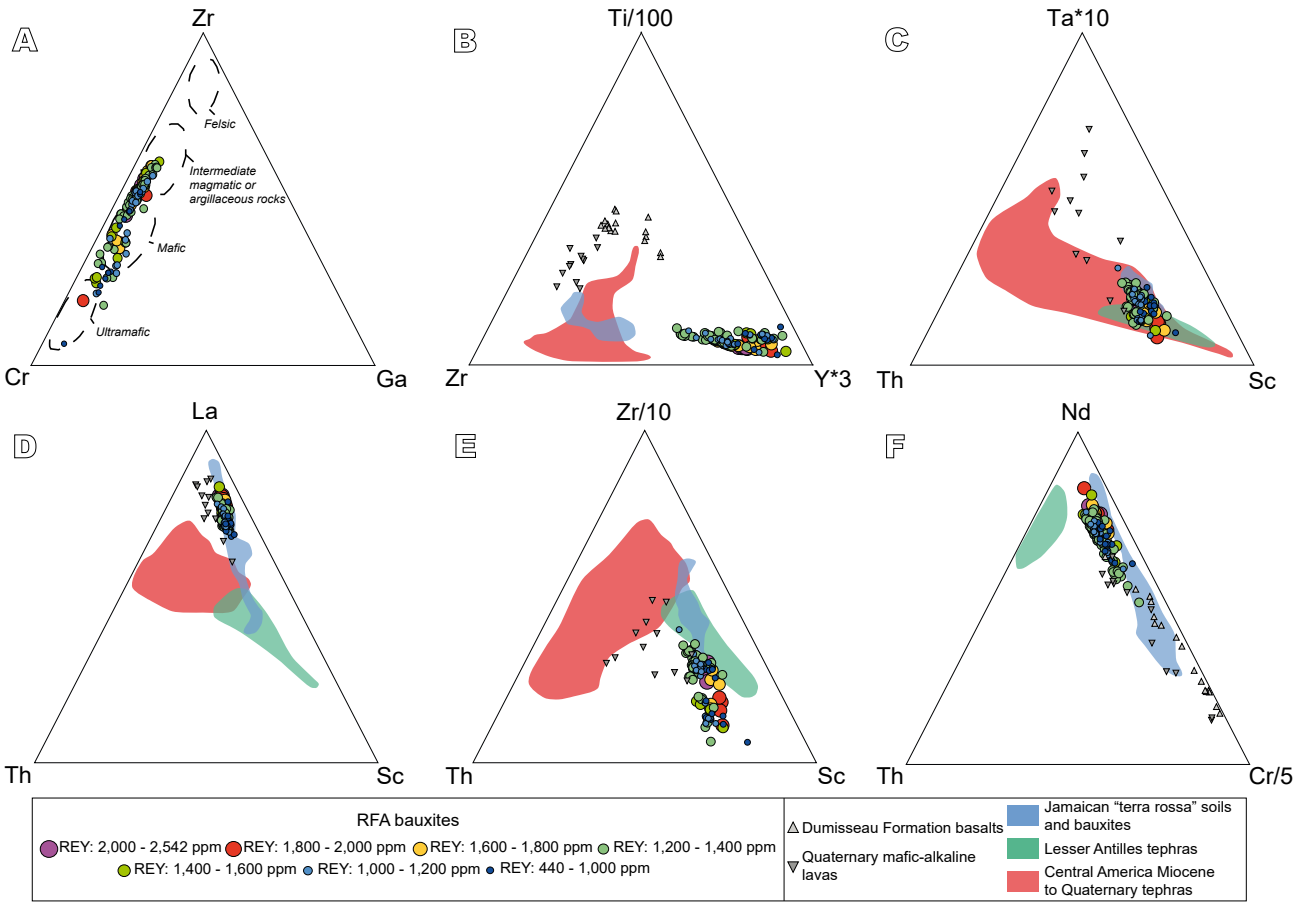

FIGURE 11. Ternary compositional diagrams A) Zr-Cr-Ga, with compositional fields after Özlü (1983) and Reinhardt *et al.* (2018). B) Ti/100-Zr-Y*3. C) Ta*10-Th-Sc. D) La-Th-Sc. E) Zr/10-Th-Sc. F) Nd-Th-Cr/5. Compositional fields in (B-F) are after Muhs and Budahn (2009). Data are compared to Dumisseau Formation basalts (Escuder-Viruete *et al.*, 2016), Quaternary mafic-alkaline lavas from La Hispaniola (Kamenov *et al.*, 2011), Jamaican "terra rossa" soils and bauxites (Muhs and Budahn, 2009), Lesser Antilles tephras (Muhs *et al.*, 2007), and Central America Miocene to Quaternary tephras (Schindlbeck *et al.*, 2018).

and other minor elements such as Ti and REY, which are normally found only in small amounts in the host limestone. For example, the average REY content of carbonates hosting bauxites in Bahoruco is ~25ppm (Torró *et al.*, 2017). Mass balance calculations indicate unplausible degrees of carbonate dissolution to be the source material of karst bauxites, thus precluding the limestones as exclusive and even significant contributors (Muhs and Budahn, 2009). Consequently, external sources, such as volcanic ash (*e.g.* Lyew-Ayee, 1986), debris from basement rocks (*e.g.* Bárdossy, 1982), lateritic clays (*e.g.* Yuste *et al.*, 2015), and other wind-borne material (*e.g.* Pye, 1988), have been traditionally invoked to explain the anomalous geochemistry of karst bauxites. In the case of karst bauxites in Bahoruco, Torró *et al.* (2017) suggested, based on mineralogical evidence, that the source material of the bauxites could derive from either the basalts of the Dumisseau Formation or volcanic ash deposited on the emerged Eocene-Pliocene carbonate series.

Notwithstanding the fractionation of major and trace elements that takes place during bauxitization (MacLean *et al.*, 1997; Nesbitt, 1979), the relative abundances of certain elements that are immobile at near-surface environments (*i.e.* Ti, Zr, Y, Cr, Sc, Ta, La, Nd, Ga) have been extensively utilized to ascertain potential parent materials and its provenance (Muhs and Budahn, 2009; Pearce and Cann, 1973). The composition of the studied bauxites from the RFA, as indicated in terms of Zr-Cr-Ga, is consistent with derivation from intermediate to mafic magmatic rocks (Fig. 11A). The trace element composition of the studied basalts differs from that of the Dumisseau Formation basalts (Escuder-Viruete *et al.*, 2016) and Quaternary mafic-alkaline lavas associated with the Enriquillo-Plantain Garden Fault Zone to the north of the Bahoruco (Kamenov *et al.*, 2011) (Fig. 11B-F). In addition, the trace elements composition would also disfavor Miocene to Present volcanism along Central America and the Lesser Antilles as sources of the RFA bauxites. Conversely, bauxites from the RFA plot near the fields defined by Jamaican bauxites and "terra rossa" soils, suggesting similar sources (Fig. 11B-F). The only difference between both datasets involves higher Y in the bauxites from the RFA relative to those from Jamaica (Fig. 11B). In conclusion, it is probable that Jamaican and RFA bauxites have a similar parental source. However, the ultimate source rock remains undetermined based on the current available data.

Geochemical patterns and exploration tools

The results of a Principal Component Analysis (PCA) conducted on the whole rock geochemistry of the studied bauxites show that only the first two components, PC1 and PC2, have eigenvalues exceeding 1. Consequently, the variance of the system can be adequately explained by these two components (Fig. 12A). Combined, the first two components account for 77.7% of the total variance of the dataset. The PC2 reflects the antithetic behavior of Al_2O_3 with SiO_2 and K_2O in the bauxites under study (Fig. 12B), tendency also observed in the binary diagrams from Figure 7A and 7B. The samples yielded a broad range of Al_2O_3 and SiO_2 contents, that allows for the classification of the bauxitic material into several categories (Fig. 7). These include Fe-rich bauxites and bauxites *sensu stricto* (SiO_2-poor and Al_2O_3-rich), as well as clayey bauxites and bauxitic clays (SiO_2-rich and Al_2O_3-poor; Fig. 7). The antithetic behavior of Al_2O_3 and SiO_2 provides compelling match with the mineralogy, with the samples enriched in Al_2O_3 having higher amounts of gibbsite and/or boehmite and/or nordstrandite, and the SiO_2-rich samples being more enriched in kaolinite and/or quartz.

The observed trend from SiO_2- to Al_2O_3-rich bauxites (Fig. 7) has also a geographic correspondence within the RFA, as the bauxites from the southern area contain higher amounts of Al-oxyhydroxides in comparison to those from the northern area (Fig. 6). This shift from SiO_2- to Al_2O_3-rich samples is connected to bauxite maturation (Proenza *et al.*, 2017; Torró *et al.*, 2017; Villanova-de-Benavent *et al.*, 2023). In this process, clay minerals such as kaolinite, are steadily replaced by Al-oxyhydroxides like gibbsite (Slukin *et al.*, 2014). While it is true that gibbsite is more stable than nordstrandite, which in turn is more stable than bayerite (also an $Al(OH)_3$ polymorph) and microcrystalline gibbsite, it must be noted that gibbsite, boehmite, nordstrandite and bayerite are all metastable under surface weathering conditions (*i.e.* their occurrence is related to non-equilibrium processes; Anovitz *et al.*, 1991 and references therein). However, these phases may precipitate at different pH. Thus, according to Barnhisel and Rich (1965), gibbsite is the only phase to precipitate from solutions at pH< 4.4; at pH= 4.4-5.8, gibbsite precipitates along with nordstrandite. At pH= 5.8-7, nordstrandite and bayerite precipitate, and only bayerite precipitates at pH> 9. Besides, whether gibbsite forms as a direct replacement of a primary aluminosilicate, or through an intermediate clay mineral, depends on the formation conditions. While both processes may occur following weathering of basic to intermediate rocks under tropical to subtropical temperatures and high rainfall, the direct replacement of a primary aluminosilicate is characteristic of good drainage, whereas the replacement through an intermediate clay mineral is associated with poor drainage (Hemingway, 1982 and references therein). Regardless, the prevalent mineralogy of the karst bauxites is independent of the host carbonate and is primarily determined by physic-chemical conditions during the bauxitization process.

The variation of the other major component in the studied bauxites, Fe_2O_3, is mostly explained by the PC1

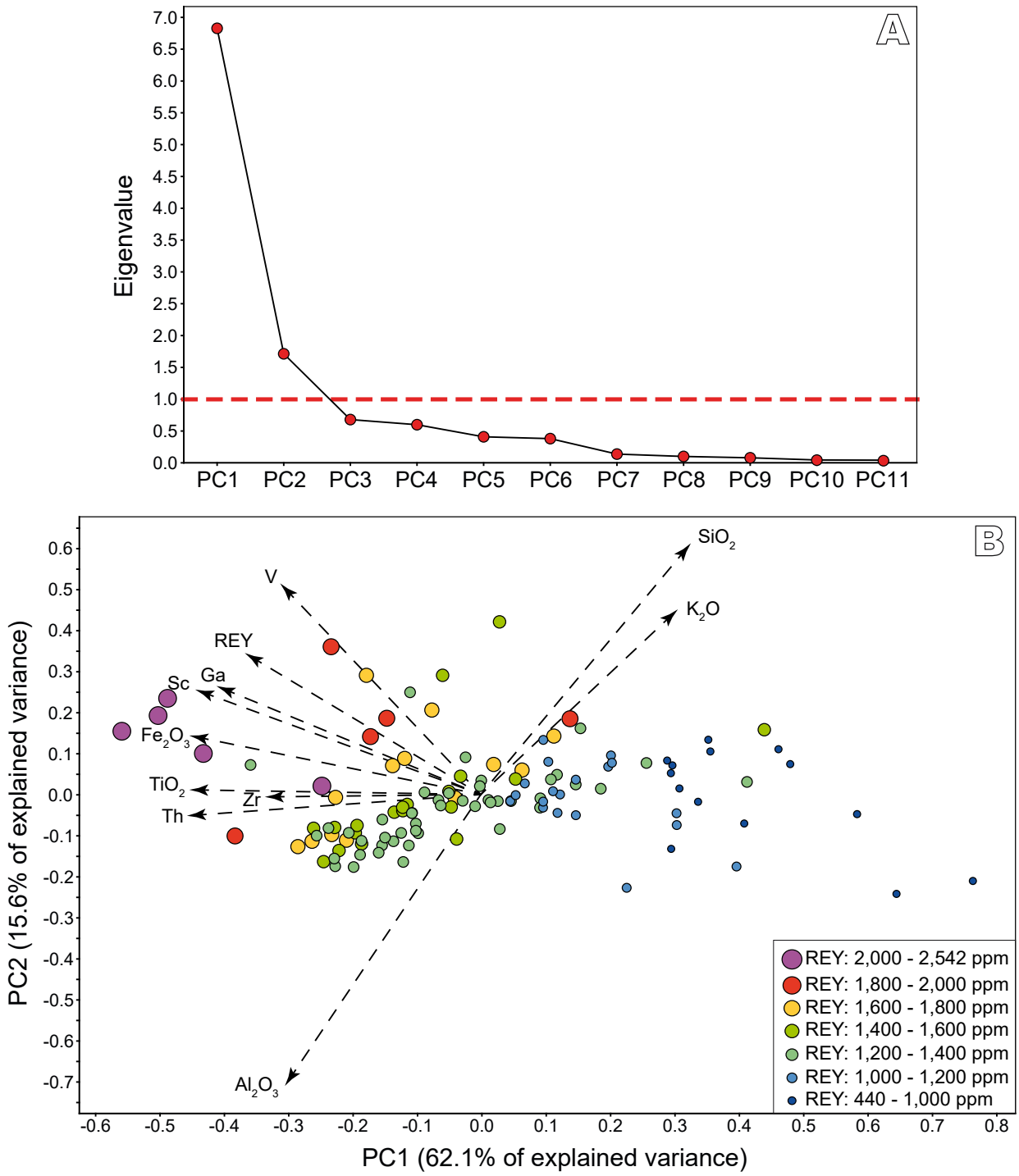

FIGURE 12. A) Scree plot showing the eigenvalues (explained variance) of each Principal Component (PCs) of the dataset. B) PC1 vs PC2 binary diagram of the studied samples.

and appears perpendicular to the trends defined by Al_2O_3 with SiO_2 and K_2O (Fig. 12B). Other minor elements, such as TiO_2, trace elements, like V, Zr and Th, and conspicuously the critical metals of interest, such as REY, Sc and Ga, exhibit a similar trend as Fe_2O_3 in the PCA. This provides compelling evidence that their content in the studied samples is independent of the degree of bauxite maturation. It is noteworthy that the REY, and other critical metals such as Sc and Ga, contents in the RFA samples are similar irrespective of their Al_2O_3 and SiO_2 contents (Figs.

8-9). This observation pinpoints that REY, Sc and Ga are equally enriched in samples with broadly different silicate-to-alumina ratios and that they did not undergo differential concentration during the bauxite maturation process.

In this line of evidence, the samples from the southern area of the RFA, which have higher Al-oxyhydroxides modal proportions and therefore are more mature, yielded lesser contents of REY compared to samples from the northern area, which are characterized by containing lesser amounts of Al-oxyhydroxides and should be catalogued as immature bauxites (Fig. 6). Consequently, the degree of bauxite maturation cannot be used in the RFA as a vector to explore REY, Sc or Ga. An alternative approach would be to utilize Th, a radioactive element that is well-correlated to REY, Sc and Ga in the studied samples (Figs. 9; 12B). Thorium contents can easily and quickly be estimated using a gamma-ray spectrometer. Likewise, K, whose isotope ^{40}K is also radioactive, is also negatively correlated with REY, Sc and Ga (Figs. 9I; 12B) and therefore could also be used during exploration. Thus, a detailed geophysical campaign using gamma-ray spectrometry on the RFA bauxites could prove advantageous to seek for the most favorable areas for REY, Sc and Ga.

REY resources of the RFA

The studied bauxites are enriched in LREE and Y compared to MREE and HREE, and consequently exhibit linear negative slope patterns in chondrite-normalized REY diagrams (Fig. 10). These characteristic patterns are also observed in Mediterranean-type karst bauxites globally. The main difference between the RFA and other Mediterranean-type bauxites resides in their REY contents (Fig. 10). The Mediterranean-type bauxites have REY contents that oscillate between 85 to 1,506ppm, with a median value of 657ppm (Deady *et al.*, 2014; Mondillo *et al.*, 2011, 2019; Mouchos *et al.*, 2016; Putzolu *et al.*, 2018; Radusinovic and Papadopoulos, 2021; Reinhardt *et al.*, 2018). On the contrary, the studied samples from the RFA exhibit considerably higher REY contents, with values ranging from 440 to 2,542ppm and a median content of 1,310ppm, doubling the one from the Mediterranean-type bauxites, thus proving the extreme REY enrichment of the RFA bauxites.

In regard to the distribution of each element of the REY in the studied bauxite samples, the most abundant are Y (~28-30% of total REY), La (~18-20%), Ce (~15-19%) and Nd (~14-15%) (Fig. 13). The remaining ~20 to 25 of the REY are composed predominantly of MREE and HREE. The proportions of these elements remain consistent and are not dependent on the total REY contents. Villanova-de-Benavent *et al.* (2023), in their study of the karst bauxite deposits of the neighboring Sierra de Bahoruco Natural Park, described an ultra-rich REY bauxite deposit, named Km-30 (mislabeled "El Turco" in the referred work), whose REY contents have an average of 2.63wt.%. The

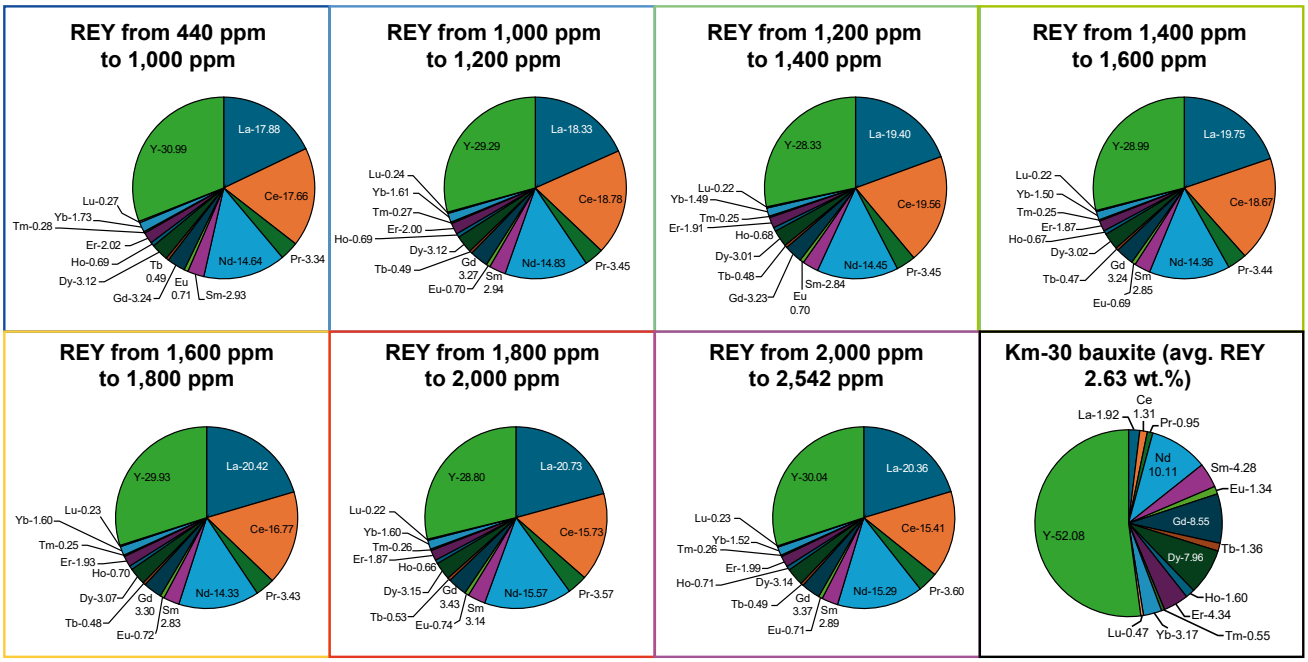

FIGURE 13. Cake diagrams showing the distribution of each element of the REY within the studied bauxite samples sorted by whole-rock total REY contents. Data for the Km-30 karst bauxite deposit (Villanova-de-Benavent *et al.*, 2023) is shown for comparison.

distribution of REY in this deposit is radically different from that observed at the RFA, as this deposit has a pronounced enrichment in MREE and HREE relative to LREE adopting a bell-like shape in their chondrite-normalized REY pattern (see Fig. 4 in Villanova-de-Benavent *et al.*, 2023). The most abundant REY elements of this deposit are Y (~52%), Nd (~10%), Gd (~9%) and Dy (~8%; Fig. 13). The extraction of REY could represent an important surplus in the economic revenue of RFA bauxite exploitation. However, given that the market values of the MREE and HREE are higher relative to that of LREE (Gielen and Lyons, 2022), it would be of great importance to explore for deposits like Km-30 within the RFA to enhance the economic significance of its bauxites.

Other critical metals and the concept of full-value mining

In addition to REY, the bauxites from the RFA are also enriched in other metals that are listed by several national and international agencies as critical, such as Sc and Ga, (*e.g.* European Commission, 2023; International Energy Agency, 2023; USGS, 2024). Scandium is most commonly found in very low contents in dozens of minerals and is currently recovered as a by-product in large scale production of other metals such as REE, Ti, Ta, Nb, U, and Ni (Mostajeran *et al.*, 2021; Yasukawa *et al.*, 2018). The economic viability of exploiting Sc as a by-product is established at contents between 20 to 50ppm (Wang *et al.*, 2011). The RFA bauxites contain Sc concentrations oscillating between 17 and 105ppm (median of 66ppm), which are very similar to the ones found in other deposits where Sc is considered as a viable commodity (*e.g.* the Moa Bay Ni laterite district, Cuba, with a median Sc content of 77ppm; Aiglsperger *et al.*, 2016; Domínguez-Carretero *et al.*, 2024).

Gallium is mostly produced as a by-product of bauxite and zinc processing (USGS, 2024). The average Ga content of bauxite that is economically viable for its exploitation is ~50ppm (USGS, 2024). The bauxite samples from the RFA have Ga contents that range from 11 to 54ppm (median of 40ppm), rendering them suitable targets for this metal.

The energy transition currently underway in many countries aiming to a shift from a carbon-based society to a society with low or zero CO_2 emissions, implies an increasing demand for certain critical metals, such as REY, Sc or Ga (*e.g.* European Commission, 2023). Hence, the opening of new mines and the re-assessment of the existing ones will be required. The strategy of "full-value mining" involves identifying new ways to produce more metal(s) out of the same mined material, thereby reducing waste while enhancing the economics of the mine (Dold, 2020). This more sustainable approach to mining can certainly be applied at the RFA with a focus on the recovery of REY with Sc and Ga.

CONCLUSIONS

The Mediterranean-type karst bauxite deposits from the state-owned Reserva Fiscal Ávila (RFA) in the Sierra de Bahoruco (SW Dominican Republic) are composed of clayey to Fe-rich bauxites, whose mineralogy consists mainly of Al-oxyhydroxides and kaolinite. The deposits contain high REY contents, with a median value of 1,310ppm and up to 2,542ppm. The contents of REY are decoupled form the degree of bauxite maturity. Our study also indicates that different bauxites from a same district may exhibit disparate REY patterns. In addition to REY, the bauxites from the RFA also have significant contents of Sc (median value of 66ppm) and Ga (median value of 40ppm). The positive correlation between the contents of these critical elements and Th, and negative correlation with K, makes gamma-ray spectrometry an appropriate tool for the exploration and early targeting of the bauxite deposits that are more prospective for their economic benefit. The contents of these critical metals confirm that karst bauxites from the Sierra de Bahoruco, including those from the RFA, are among the richest deposits of this type with regards to these elements globally. Their extraction could potentially represent a substantial economic surplus to the revenue generated solely from the aluminum production, while concurrently reducing the volume of waste.

ACKNOWLEDGMENTS

This research was financially supported by Spanish grants PID 2019-105625RB-C21 and PID2023-147788OB-I00 funded by MCIN/AEI/10.13039/501100011033. Additional funding has been provided by the MESCYT (Ministry of Higher Education, Science and Technology of the Dominican Republic) project 2022-1A4-189. This paper has been produced within the framework of the MinResET (Mineral Resources for the Energy Transition) research group (2021-SGR-00239, Agència de Gestió d'Ajuts Universitaris i de Recerca de Catalunya). We are grateful to Edwin García, Arnold Evangelista and Edwin Fajardo for their collaboration and support, and to driver Gregorio Báez (Gregory) for their inestimable help, during the field work campaigns.

REFERENCES

Aiglsperger, T., Proenza, J.A., Lewis, J.F, Labrador, M., Svojtka, M., Rojas- Purón, A., Longo, F, Ďurišová, J., 2016. Critical metals (REE, Sc, PGE) in Ni-laterites from Cuba and the Dominican Republic. Ore Geology Reviews, 73, 127-147.

Anovitz, L.A., Perkins, D., Essene, E.J., 1991. Metastability in near-surface rocks of minerals in the system Al_2O_3-SiO_2-H_2O. Clays and Clay Minerals, 39, 225-233.

Balaram, V., 2019. Rare earth elements: A review of applications, occurrence, exploration, analysis, recycling, and environmental impact. Geoscience Frontiers, 10, 1285-1303.

Bárdossy, G., 1982. Karst bauxites. Bauxite deposits on carbonate rocks. Budapest (Hungary), Elsevier, Developments in Economic Geology, 1st ed., 14, 441pp.

Barnhisel, R.I., Rich, C.I., 1965. Gibbsite, bayerite, and nordstrandite formation as affected by anions, pH, and mineral surfaces. Soil Science Society of America Journal, 29, 531-534.

Charles, N., Tuduri, J., Lefebvre, G., Pourret, O., Gaillard, F., Goodenough, K., 2021. Ressources en terres rares de l'Europe et du Groenland: un potentiel minier remarquable mais tabou? In: Boulvais, P., Decrée, S. (eds.). Ressources métalliques: cadre géodynamique et exemples remarquables. ISTE Science Publishing Ltd-Wiley, .

Chen, J., Wang, Q., Zhang, Q., Carranza, E.J.M., Wang, J., 2018. Mineralogical and geochemical investigations on the iron-rich gibbsitic bauxite in Yongjiang basin, SW China. Journal of Geochemical Exploration, 188, 413-426.

de León, O., 1989. Geología De La Sierra De Bahoruco (República Dominicana). Santo Domingo, Museo Nacional de Historia Natural, 112pp.

Deady, E., Mouchos, E., Goodenough, K., Williamson, B., Wall, F., 2014. Rare earth elements in karst-bauxites: a novel untapped European resource? ERES2014: 1st European Rare Earth Resources Conference, Milos, 1-12.

Dold, B., 2020. Sourcing of critical elements and industrial minerals from mine waste - The final evolutionary step back to sustainability of humankind? Journal of Geochemical Exploration, 219, 106638.

Domínguez-Carretero, D., Proenza, J.A., Villanova-de-Benavent, C., Aiglsperger, T., Tauler, E., Rojas-Purón, A., Duque, N., González-Jiménez, J.M., Garcia-Casco, A., Galí, S., 2024. The geology, geochemistry, and mineralogy of the Moa Bay Ni laterite mining district, Cuba. Economic Geology, 119, 1685-1706.

Escuder-Viruete, J., 2010. Mapa Geológico de la República Dominicana E. 1:50.000. Informe (Parte 1) de Petrología de Rocas Ígneas y Metamórficas, Hojas de Polo, La Ciénaga, Enriquillo, Sabana Buey y Nizao. Santo Domingo, Dirección General de Minería.

Escuder-Viruete, J., Joubert, M., Abad, M., Pérez-Valera, F., Gabites, J., 2016. The basaltic volcanism of the Dumisseau Formation in the Sierra de Bahoruco, SW Dominican Republic: A record of the mantle plume-related magmatism of the Caribbean Large Igneous Province. Lithos, 254-255, 67-83.

European Commission, 2023. Study on the Critical Raw Materials for the EU (Final Report). Brussels, European Commission, 158pp.

Gielen, D., Lyons, M., 2022. Critical Materials for the Energy Transition: Rare Earth Elements. Abu Dhabi, International Renewable Energy Agency, 48pp.

Goodenough, K.M., Wall, F., Merriman, D., 2017. The Rare Earth Elements: Demand, Global Resources, and Challenges for Resourcing Future Generations. Natural Resources Research, 27, 201-216.

Hemingway, S., 1982. Gibbs Free Energies of Formation for Bayerite, Nordstrandite, $A1(OH)^{2+}$, and $A1(OH)_2{}^{+}$, Aluminum Mobility, and the Formation of Bauxites and Laterites. In: Saxena, S.K. (eds.). Advances in Physical Geochemistry. New York, Springer, Advances in Physical Geochemistry, 2,

Herrington, R., 2021. Mining our green future. Nature Reviews Materials, 6, 456-458.

International Energy Agency, 2023. Critical Minerals Market Review 2023. Paris, International Energy Agency, 84pp.

International Renewable Energy Agency, 2023. Geopolitics of the energy transition. Critical materials. Abu Dhabi, International Renewable Energy Agency, 150pp.

Kamenov, G.D., Perfit, M.R., Lewis, J.F., Goss, A.R., Arévalo R.Jr., Shuster, R.D., 2011. Ancient lithospheric source for Quaternary lavas in Hispaniola. Nature Geoscience, 4, 554-557.

Lidiak, E.G., Anderson, T.H., 2015. Evolution of the Caribbean plate and origin of the Gulf of Mexico in light of plate motions accommodated by strike-slip faulting. In: Anderson, T.H., Didenko, A.N., Johnson, C.L., Khanchuk, A.I., MacDonald, J.H.Jr. (eds.). Late Jurassic Margin of Laurasia-A Record of Faulting Accommodating Plate Rotation. Boulder (Colorado, United States of America), Geological Society of America, Special Paper, 513, SPE513-01.

Liu, S.L., Fan, H.R., Liu, H., Meng, J., Butcher, A.R., Yann, L., Yang, K.F., Li, X.C., 2023. Global rare earth elements projects: New developments and supply chains. Ore Geology Reviews, 157, 105428.

Lyew-Ayee, P.A., 1986. A case for the volcanic origin of Jamaican bauxites. Kingston (Jamaica), Proceedings of the Bauxite Symposium VI, 30pp.

MacLean, W.H., Bonavia, F.F., Sanna, G., 1997. Argillite debris converted to bauxite during karst weathering: Evidence from immobile element geochemistry at the Olmedo Deposit, Sardinia. Mineralium Deposita, 32, 607-616.

Mann, P., 2007. Overview of the tectonic history of northern Central America. Geological Society of America, Special Papers, 428, 1-19.

Mendoza-Ulloa, F., Rodríguez-Reyes, J., Vargas, J., Agramonte, K., Garcia-Cocco, E.R., 2023. Mapa con los depósitos de bauxitas evaluados, explorados y explotados por la ALCOA. República Dominicana, Servicio Geológico Nacional.

Mondillo, N., Balassone, G., Boni, M., Rollinson, G., 2011. Karst bauxites in the Campania Apennines (southern Italy): a new approach. Periodico di Mineralogia, 80, 407-432.

Mondillo, N., Balassone, G., Boni, M., Chelle-Michou, C., Cretella, S., Moromone, A., Putzolu, F., Santoro, L., Scognamiglio, G., Tarallo, M., 2019. Minerals, 9, 504.

Moseley, G.E., Richards, D.A., Smart, P.L., Standish, C.D., Hoffmann, D.L., Hove, H., Vinn, O., 2015. Early-middle

Holocene relative sea-level oscillation events recorded in a submerged speleothem from the Yucatán Peninsula, Mexico. Holocene, 25, 1511-1521.

Mostajeran, M., Bondy, J.M., Reynier, N., Cameron, R., 2021. Mining value from waste: Scandium and rare earth elements selective recovery from coal fly ash leach solutions. Minerals Engineering, 173, 107091.

Mouchos, E., Wall, F., Williams, B.J., Palumbo-Roe, B., 2016. Easily leachable rare earth element phases in the Parnassus-Giona bauxite deposits, Greece. Bulletin of the Geological Society of Greece (L), 1952-1958.

Muhs, D.R., Budahn, J.R., 2009. Geochemical evidence for African dust and volcanic ash inputs to terra rossa soils on carbonate reef terraces, northern Jamaica, West Indies. Quaternary International, 196, 13-35.

Muhs, D.R., Budahn, J., Prospero, J.M., Carey, S.N., 2007. Geochemical evidence for African dust inputs to soils of western Atlantic islands: Barbados, the Bahamas and Florida. Journal of Geophysical Research, 112, F02009.

Nesbitt, H.W., 1979. Mobility and fractionation of rare earth elements during weathering of a granodiorite. Nature, 279, 206-210.

Özlü, N., 1983. Trace-element content of "Karst Bauxites" and their parent rocks in the mediterranean belt. Mineralium Deposita, 18, 469 - 476.

Pearce, J.A., Cann, J.R., 1973. Tectonic setting of basic volcanic rocks determined using trace element analyses. Earth and Planetary Science Letters, 19, 290-300.

Pérez-Valera, F., 2010. Geologic Map Sheet 1:50.000 num. 5970-III and corresponding memoir. Proyecto 1B de Cartografía Geotemática de la República Dominicana. Programa SYSMIN. Santo Domingo, Dirección General de Minería.

Pérez-Valera, F., Abad, M., 2010. Informe Estratigráfico y Sedimentológico. Proyecto 1B de la Cartografía Geotemática de la República Dominicana. Programa SYSMIN. Santo Domingo, Dirección General de Minería.

Proenza, J.A., Aiglsperger, T., Villanova-de-Benavent, C., Torró, L., Rodríguez, D., Ramírez, A., Rodríguez, J., 2017. Discovery of REE minerals hosted in karst bauxite ores from the Sierra de Bahoruco, Pedernales, Dominican Republic. Québec City (Canada), Proceedings of the 14th SGA Biennial Meeting, 4, 1321-1324.

Putzolu, F., Papa, A.P., Mondillo, N., Boni, M., Balassone, M., Moromone, A., 2018. Geochemical Characterization of Bauxite Deposits from the Abruzzi Mining District (Italy). Minerals, 8, 298.

Pye, K., 1988. Bauxites gathering dust. Nature, 333, 800-801.

Radusinovic, S., Papadopoulos, A., 2021. The Potential for REE and Associated Critical Metals in Karstic Bauxites and Bauxite Residue of Montenegro. Minerals, 11, 295.

Reinhardt, N., Proenza, J.A., Villanova-de-Benavent, C., Aiglsperger, T., Bover-Arnal, T., Torró, L., Salas, R., Dziggel, A., 2018. Geochemistry and mineralogy of rare earth elements (REE) in bauxitic ores of the Catalan Coastal Range, NE Spain. Minerals, 8, 562.

Schindlbeck, J.C., Kutterolf, S., Freundt, A., Eisele, S., Wang, K.L., Frische, M., 2018. Miocene to Holocene Marine Tephrostratigraphy Offshore Northern Central America and Southern Mexico: Pulsed Activity of Known Volcanic Complexes. Geochemistry, Geophysics, Geosystems, 19, 4143-4173.

Slukin, A.D., Bortnikov, N.S., Zhegallo, E.A., Zhukhlistov, A.P., Boeva, N.M., 2014. Gibbsite and Kaolinite in the Biological Pedoturbation Zone of the Lateritic Profile: A Different Fate (Exemplified by Deposits of Siberia, India, Guinea, and Brazil). Doklady Earth Sciences, 458, 1220-1225.

Thompson, W.G., Curran, H.A., Wilson, M.A., White, B., 2011. Sea-level oscillations during the last interglacial highstand recorded by Bahamas corals. Nature Geosciences, 4, 684-687.

Torró, L., Proenza, J.A., Aiglsperger, T., Bover-Arnal, T., Villanova-de-Benavent, C., Rodríguez-García, D., Ramírez, A., Rodríguez, J., Mosquea, L.A., Salas, R., 2017. Geological, geochemical and mineralogical characteristics of REE-bearing Las Mercedes bauxite deposit, Dominican Republic. Ore Geology Reviews, 89, 114-131.

USGS, 2024. United States Geological Survey, Mineral Commodity Summaries, 216 pp.

Villanova-de-Benavent, C., Proenza, J.A., Torró, L., Aiglsperger, T., Domènech, C., Domínguez-Carretero, D., Llovet, X., Suñer, P., Ramírez, A., Rodríguez, J., 2023. REE ultra-rich karst bauxite deposits in the Pedernales Peninsula, Dominican Republic: Mineralogy of REE phosphates and carbonates. Ore Geology Reviews, 157, 105422.

Wang, W., Pranolo, Y., Cheng, C.Y., 2011. Metallurgical processes for scandium recovery from various resources: A review. Hydrometallurgy, 108, 100-108.

Yasukawa, K., Ohta, J., Mimura, K., Tanaka, E., Takaya, Y., Usui, Y., Fujinaga, K., Machida, S., Nozaki, T., Iijima, K., Nakamura, K., Kato, Y., 2018. A new and prospective resource for scandium: Evidence from the geochemistry of deep-sea sediment in the western North Pacific Ocean. Ore Geology Reviews, 102, 260-267.

Yuste, A., Bauluz, B., Mayayo, M.J., 2015. Genesis and mineral transformations in Lower Cretaceous karst bauxites (NE Spain): Climatic influence and superimposed processes: Lower Cretaceous Karst Bauxites. Geological Journal, 50, 839-857.

Manuscript received August 2024;
revision accepted February 2025;
published Online May 2025.